Confinement and pedestal in dimensionless collisionality scans of low triangularity H-mode plasmas in JET-ILW

L. Frassinetti[1], M. N. A. Beurskens[2], S. Saarelma[2], J. E. Boom[3], E. Delabie[4], J. Flanagan[2], C. M. Kempenaars[2], Giroud[2], P. Lomas[2], L. Meneses[5], S. Menmuir[2], I. Nunes[5], F. Rimini[2], and JET contributors*

EUROfusion Consortium, JET, Culham Science Centre, Abingdon, OX14 3DB, UK

[1]Division of Fusion Plasma Physics, KTH Royal Institute of Technology, Stockholm SE

[2]CCFE, Culham Science Centre, Abingdon,OX14 3DB, UK

[3]Max-Planck-Institut für Plasma Physik, Boltzmannstr.2, 85748 Garching, Germany

[4]Oak Ridge National Laboratory, Oak Ridge, TN 37831-6169 USA

[5]Instituto de Plasmas e Fusão Nuclear, Universidade de Lisboa, 1049-001 Lisboa, Portugal

** See the Appendix of F. Romanelli et al., Proceedings of the 25th IAEA Fusion Energy Conference 2014, Saint Petersburg, Russia*

INTRODUCTION

The baseline type I ELMy H-mode scenario with H=1 has been re-established in JET with the new tungsten divertor and beryllium main wall (JET-ILW) in 2011. Comparing carbon wall (JET-C) discharges in similar conditions, a degradation of the confinement has been observed in JET-ILW, with the reduction mainly driven by a lower pedestal pressure [1]. Results presented in [2,3,4,5] show that JET-ILW at low collisionality (ν*) reaches a confinement comparable to the JET-C. The present work describes the results on the confinement and on the pedestal of a dimensionless collisionality scan.

THE DATA SET

The collisionality scan is obtained in baseline JET-ILW plasmas by allowing to vary power, current and gas in the range P_{NBI}≈11-22MW, I_p≈1.5-2.5MA and $\Gamma_{D2}\approx 1\text{-}6\cdot 10^{22}$ (e/s). The safety factor and the triangularity are kept constant at $q_{95}\approx 3$ and δ≈0.22. The volume averaged collisionality ⟨ν*⟩, defined as

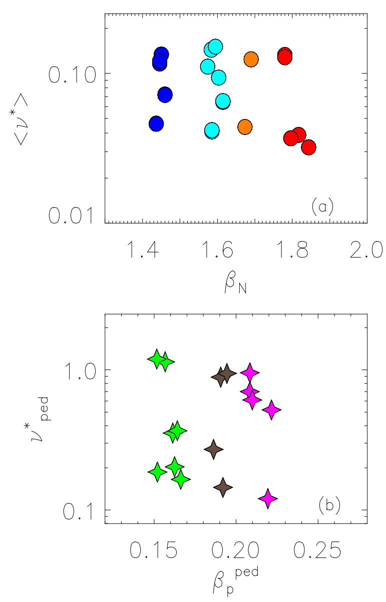

Figure 1. Range of dimensionless parameters used. The colours highlight data with similar β_N (a) and similar pedestal β_θ (b).

the ion-electron collision frequency normalized to the bounce frequency, $\nu^*=6.9\cdot10^{-18}n_eRq_{95}Z_{eff}\ln\Lambda/(\varepsilon^{3/2}T_e^2)$, is varied by a factor 5. Four collisionality scans obtained at four different β_N values have been performed. The parameters range is shown in figure 1(a). The volume averaged normalized ion poloidal Larmor radius is kept constant at $\langle\rho^*\rangle\approx2.4$-$2.7\%$. This dataset is used to investigate the dependence of the global confinement on the collisionality. However, the change in collisionality affects the density peaking, therefore, a dataset with constant β_N has different pedestal beta. For this reason, figure 1(b) shows a dataset [whose shots are mostly the same as those in figure 1(a)] in which the plasmas with constant pedestal β_θ have been highlighted. The corresponding ν^* varies by a factor 10 at the pedestal, while ρ^* at the pedestal is constant at $\rho^*_{ped}\approx1.6$-1.8%. This dataset is used when discussing the pedestal structure.

CONFINEMENT

The confinement factor versus the normalized beta is shown in figure 2(a). The dashed line shows the typical trend between H_{98} and β_N in JET-C. The ν^* scans of the JET-ILW data show a more complex behaviour. The high ν^* JET-ILW plasmas have low confinement ($H_{98}\approx0.8$), while at low ν^* JET-ILW reaches confinement comparable to JET-C. The improvement from high to low ν^* is more evident at high β_N than at low β_N (compare the blue and the red dots in figure 1a). The trend of H_{98} and total stored energy versus $\langle\nu^*\rangle$ are shown in figures 2(b) and 2(c) respectively. The increase of H_{98} and W_{th} with the reduction of collisionality is clear.

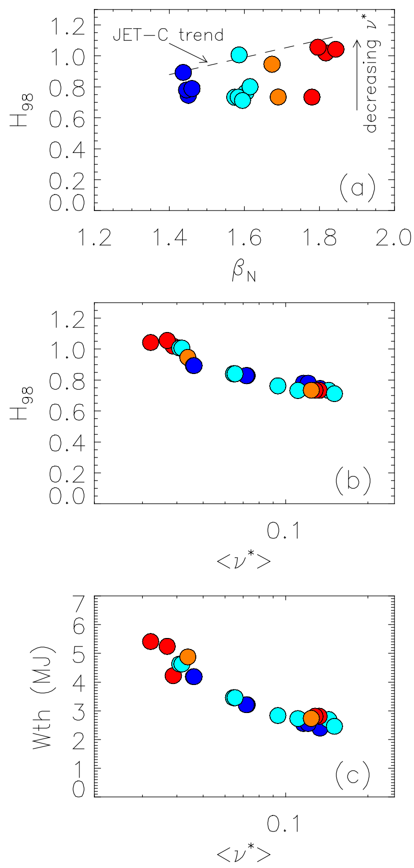

Figure 2. Confinement factor versus β_N (a) and versus collisionality (b). Total thermal energy versus collisionality. Colour code as in figure 1(a).

The increase in W_{th} is due to both the increase of the pedestal pressure and of the core pressure, as described in figure 3. Figure 3(a) shows the pedestal electron temperature T_e^{ped} versus the pedestal electron density n_e^{ped}. Reducing ν^* in the JET-ILW dimensionless collisionality scan produces a decrease of n_e^{ped} and an increase of T_e^{ped}. The T_e^{ped} increase is stronger than the n_e^{ped}

reduction, so a higher pedestal pressure is obtained (P_e^{ped}≈4kPa at high ν* and P_e^{ped}≈6kPa at low ν*). In the core, figure 3(b), the density does not change significantly, while the temperature increases from ≈2.5keV to ≈5keV and consequently the pressure from ≈25kPa to ≈45-50kPa.

The change in collisionality strongly affects the peaking [2,6], as shown in figure 4(a). The T_e peaking remains constant, as shown in figure 4(b), so the pressure peaking increases at low collisionality.

Therefore, the increase of the W_{th} with the ν* reduction is due to (1) the increase in the pedestal W_{th} due to the increase in P_e^{ped} (≈50%) and to (2) the increase in the core W_{th} (≈75%) due to the increase in P_e peaking and to the T_e profile stiffness.

PEDESTAL STRUCTURE and EPED RESULTS

Recent experimental results [4] show that the pedestal pressure width w_{pe} in JET-ILW scales with the pedestal β_θ., as observed in other devices and predicted by the KBM model. In this work, w_{pe} is estimated as the average between T_e and n_e pedestal widths, in agreement with the definition in EPED. Figure 5(a) shows the correlation of w_{pe} with ν*. A positive trend is observed. This is in reasonable agreement with what recently described in [7], where the width is observed to increase at high gas level. The present data at low ν* are in agreement with the EPED results based on the KBM predictions [$w_{pe}=0.076(\beta_\theta^{ped})^{0.5}$≈0.03] as shown in figure 5(b). The deviation from the prediction at high ν* suggests that the present models are not sufficient to describe in detail the pedestal width behaviour.

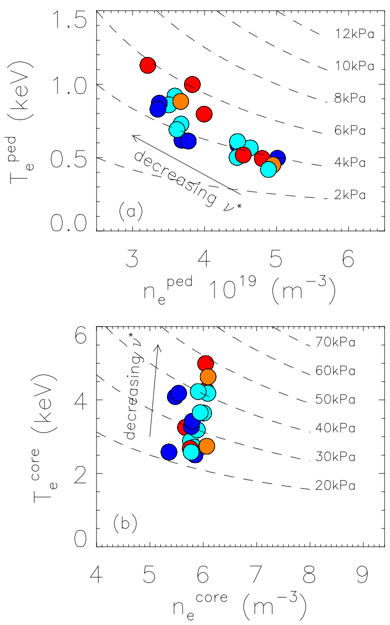

Figure 3. Electron temperature versus electron density at the pedestal (a) and in the core (b). Dashed lines highlight the isobar curves. Colour code as in figure 1(a).

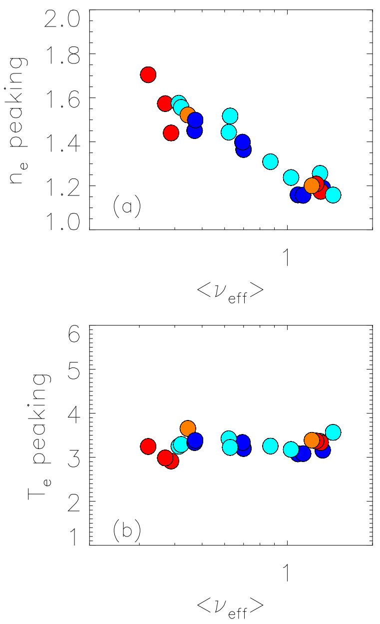

Figure 4. Density peaking (a) and temperature peaking (b) versus effective collisionality. Colour code as in fig 1(a).

The EPED results for the pedestal temperature is shown in figure 6. The EPED modelling has been performed in order to match the ρ^*_{ped} (≈1.7%) and β_θ^{ped} (≈0.15) of the JET-ILW ν* scan. EPED correctly reproduces the qualitative behaviour of the pedestal height with the ν*, but overestimates the experimental T_e^{ped} by ≈10% at high ν* and ≈15-20% at low ν*. The EPED results are consistent with the fact that the present JET-ILW plasmas are far from the stability boundary, figure 6(b).

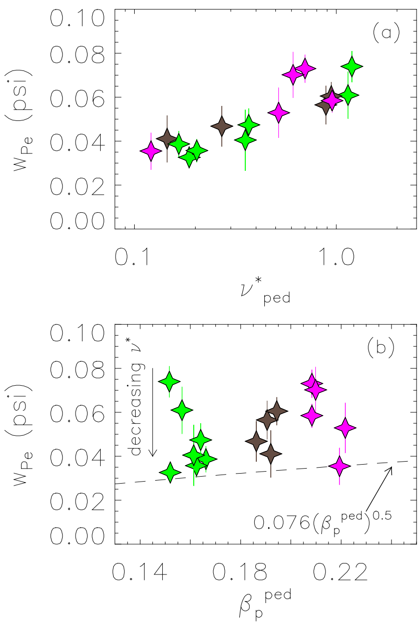

Figure 5. Pressure pedestal width versus pedestal collisionality (a) and beta poloidal (a). Colour code as in figure 1(b).

CONCLUSIONS

The work shows that JET-ILW at low collisionality can reach confinement comparable to JET-C. The high stored energy is achieved by both the increased pedestal pressure (≈50%) and by the increased core pressure (≈75%). It was not possible to find a perfect match between the present data set and JET-C (in terms of ν*,ρ*,β_θ and q_{95}), so a quantitative comparison cannot be done, but, qualitatively, JET-C and JET-ILW have similar trends with collisionality.

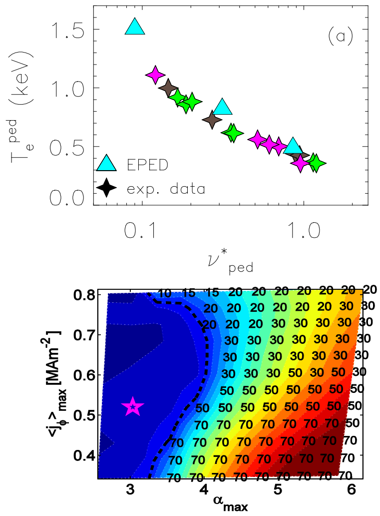

*Figure 6. Pedestal temperature versus ν^*_{ped} for experimental data and EPED simulations (a). Stability diagram for a low ν*plasma (b).*

ACKNOWLEDGEMENT

This work has been carried out within the framework of the EUROfusion Consortium and has received funding from the Euratom research and training programme 2014-2018 under grant agreement No 633053. The views and opinions expressed herein do not necessarily reflect those of the European Commission.”

REFERENCES

[1] C. Giroud et al., Nucl. Fusion **53** 113025 (2013)
[2] M. Beurskens et al., Nucl. Fusion **54** 043001 (2014)
[3] C. Challis et al., Nucl. Fusion **55** 053031 (2015)
[4] C. Maggi et al., submitted to Nucl. Fusion
[5] I. Nunes et al., 25th IAEA Fusion Energy Conf. (S. Petersburg, 2014) EX/9-2
[6] M. Maslov et al., Nucl. Fusion **49** 075037 (2009)
[7] M. Leyland et al., Nucl Fusion **55** 013019 (2015)